PCCP

COMMUNICATION

View Article Online
View Journal | View Issue

Check for updates

Cite this: *Phys. Chem. Chem. Phys.*, 2017, **19**, 17531

Received 21st April 2017,
Accepted 21st June 2017

DOI: 10.1039/c7cp02635h

rsc.li/pccp

Published on 21 junio 2017. Downloaded by Fail Open on 23/07/2025 9:10:29.

Water–chromophore electron transfer determines the photochemistry of cytosine and cytidine†

Rafał Szabla, *[ab] Holger Kruse,[b] Jiří Šponer[b] and Robert W. Góra[c]

Many of the UV-induced phenomena observed experimentally for aqueous cytidine were lacking the mechanistic interpretation for decades. These processes include the substantial population of the puzzling long-lived dark state, photohydration, cytidine to uridine conversion and oxazolidinone formation. Here, we present quantum-chemical simulations of excited-state spectra and potential energy surfaces of *N*1-methylcytosine clustered with two water molecules using the second-order approximate coupled cluster (CC2), complete active space with second-order perturbation theory (CASPT2), and multireference configuration interaction with single and double excitation (MR-CISD) methods. We argue that the assignment of the long-lived dark state to a singlet nπ* excitation involving water–chromophore electron transfer might serve as an explanation for the numerous experimental observations. While our simulated spectra for the $n\pi^*_{CT}$ state are in excellent agreement with experimentally acquired data, the electron-driven proton transfer process occurring on the $n\pi^*_{CT}$ surface may initiate the subsequent damage in the vibrationally hot ground state of the chromophore.

The molecular mechanism of ultrafast photorelaxation in UV-excited cytosine was first proposed in 2002 and assigned to the existence of an $n\pi^*/S_0$ conical intersection.[1] Even though many more works describing the excited-state dynamics of this molecule in the gas phase have appeared since then,[2–6] still little is known about the rich photoreactivity of cytosine and cytidine in aqueous environments. For instance, the mechanism governing cytidine photohydration, the primary photodamage reported for this nucleoside,[7,8] has not been explained yet. Furthermore, the most plausible photochemical reactions yielding pyrimidine nucleosides under prebiotically plausible conditions remain largely unclear from the mechanistic point of view. These include cytidine (C) to uridine (U) conversion, photoanomerisation, photoepimerization, nucleobase loss and oxazolidinone formation reactions observed by Sutherland and co-workers during the irradiation of ribonucleosides.[9–13]

Time-resolved (TR) pump probe experiments performed for cytidine in aqueous solution demonstrated a characteristic feature in the excited-state dynamics of this molecule, which was found neither in the gas phase nor in chloroform.[14,15] TR-IR spectroscopic studies performed for 5′-deoxycytidine monophosphate (CMP) in D_2O revealed the occurrence of a long-lived dark state having a distinctive band at 1574 cm^{-1} which decayed with a lifetime of 39 ± 5 ps.[16,17] This dark state was also tracked by means of transient-absorption (TA) UV techniques and a similar time constant of 34 ± 5 ps was obtained for CMP using an equivalent photoexcitation wavelength of 267 nm.[18] These measurements were tentatively attributed to the lowest-energy $^1n\pi^*$ state; however, this assignment was eventually not confirmed. In particular, theoretical simulations performed for the $^1n\pi^*$ state of 1-methylcytosine (mC) did not reproduce the characteristic TR-IR marker bands and no other evidence was provided to confirm this hypothesis.[16,17] More recent works describing nonadiabatic molecular dynamics simulations of isolated cytosine suggested that the lowest-lying triplet state of $^3\pi\pi^*$ character could be accessed with over 20% efficiency.[5,6] Therefore, it is tempting to consider the population of the $^3\pi\pi^*$ state as an alternative explanation for this phenomenon. These findings, however, are in contradiction with experimental measurements for aqueous cytidine, indicating that the triplet quantum yields do not exceed 2%.[19,20]

We anticipate that the unequivocal assignment of the character and properties of this long-lived dark state might be the key to demystifying the uncharted photoreaction mechanisms mentioned in the first paragraph. Here, we propose that the

[a] *Institute of Physics, Polish Academy of Sciences, Al. Lotników 32/46, PL-02668 Warsaw, Poland*
[b] *Institute of Biophysics, Academy of Sciences of the Czech Republic, Královopolská 135, 61265, Brno, Czech Republic. E-mail: szabla@ibp.cz*
[c] *Department of Physical and Quantum Chemistry, Wroclaw University of Science and Technology, Wybrzeże Wyspiańskiego 27, 50-370 Wrocław, Poland*

† Electronic supplementary information (ESI) available: A movie showing the molecular mechanism of the EDPT process, vibrational frequencies of the T_1 state, assignment of experimental TR-IR peaks, additional PE profiles, geometries of C–, mC– and cytidine–water clusters, vertical excitation energies from the S_1 and T_1 minima, analysis of the CASVB results and description of the methodology. See DOI: 10.1039/c7cp02635h

Published on 21 junio 2017. Downloaded by Fail Open on 23/07/2025 9:10:29.

UV-induced water–chromophore electron transfer (WCET) process, recently observed for microhydrated 7*H*-adenine,[21] serves as a single explanation for all the phenomena and ambiguities described above. For this purpose, we perform state-of-the-art quantum chemical calculations and spectral simulations using the CC2, CASPT2 and MR-CISD methods, which enable the reinterpretation of previously acquired experimental data.

Recent theoretical works revealed that water molecules could be directly involved in the formation of state crossings and significantly influence the available photorelaxation mechanisms in biomolecular building blocks.[21–26] Therefore, the inclusion of explicit water molecules, described on an equal footing with the chromophore moiety, is indispensable to correctly reproduce aqueous phase photochemistry. Fig. 1 presents the minimum-energy geometries of mC clustered with two water molecules optimized in the ground, S_1 and T_1 electronic states using the MP2/cc-pVTZ or CC2/cc-pVTZ methods. The ground state (S_0) minimum shows a regular hydrogen bonding pattern between the carbonyl and amino groups of mC and the H_2O molecules, which is also retained during the optimization of the T_1 minimum. The minimum-energy geometry of the chromophore in the T_1 state is characterized by a puckered aromatic ring with a C2–N3═C4–C5 angle of 51.9°. Such non-planarity of the hetero-aromatic ring is typical for ππ* excitations, and the associated orbitals confirm the ^{3}ππ* character of the T_1 state.

The arrangement of water molecules in the S_1 minimum of the mC–$(H_2O)_2$ cluster is significantly different from its S_0 and T_1 equilibrium geometries. The most striking feature is the strong interaction between the H_2O oxygen atom and the N3 atom of mC. The corresponding distance of 2.09 Å is considerably shorter than typical $H_2O\cdots$N3 distances in the electronic ground state, where a hydrogen bond with the amino group is expected instead (*cf.* Fig. 1). This distinctive $H_2O\cdots$N3 interaction is the result of a charge transfer equal to ∼0.24 electron from the water cluster to the chromophore moiety and was already observed in the minor 7*H*-tautomer of adenine.[21] According to the molecular orbitals presented in Fig. 2, this state can be classified as an $^1n\pi^*_{CT}$ excitation.

It is worth noting here that we show this phenomenon for the first time in a biologically relevant tautomer of a nucleobase. We also located analogous S_1 minima for the corresponding cytosine–$(H_2O)_2$ and cytidine–$(H_2O)_2$ clusters. The applicability of the CC2 method was verified through optimization of the $^1n\pi^*_{CT}$ state in the analogous cytosine–$(H_2O)_2$ cluster using the CASPT2/6-31G* approach and the resulting CC2 and CASPT2 geometries are in very good agreement (see Fig. 1 and the ESI† for more details). In addition, the $^1n\pi^*_{CT}$–S_0 energy gap at the CC2 optimized S_1 minimum of the mC–$(H_2O)_2$ cluster amounts to 1.54 eV and is quantitatively consistent with the CASPT2/cc-pVTZ-DK single-point calculation, which yielded 1.57 eV.

The WCET process occurs only after UV-excited mC relaxes to the corresponding minimum on the S_1 hypersurface described above. However, the $^1n\pi^*_{CT}$ state responsible for this charge transfer event can be associated with the $n_N\pi^*$ excitation in the Franck–Condon region, owing to the substantial involvement of the n_N molecular orbital in both cases (see the vertical excitation energies of the mC–$(H_2O)_2$ in Table 1 and Fig. 2). Vertical transition to this $n_N\pi^*$ state is characterized by a rather low oscillator strength (6.49×10^{-3}), but it can be efficiently accessed from one of the optically bright ππ* states, either S_1 or S_3. In case the lower ππ* state is populated during UV-excitation, the chromophore may change the S_1 excited-state character to the dark $^1n\pi^*_{CT}$ state during the initial relaxation on the S_1 hypersurface (see Fig. S3 in the ESI† for the corresponding PE profile). This behavior was already observed experimentally for cytosine and cytidines, and the induced fluorescence typical for bright ππ* excitations was reported only during the initial few

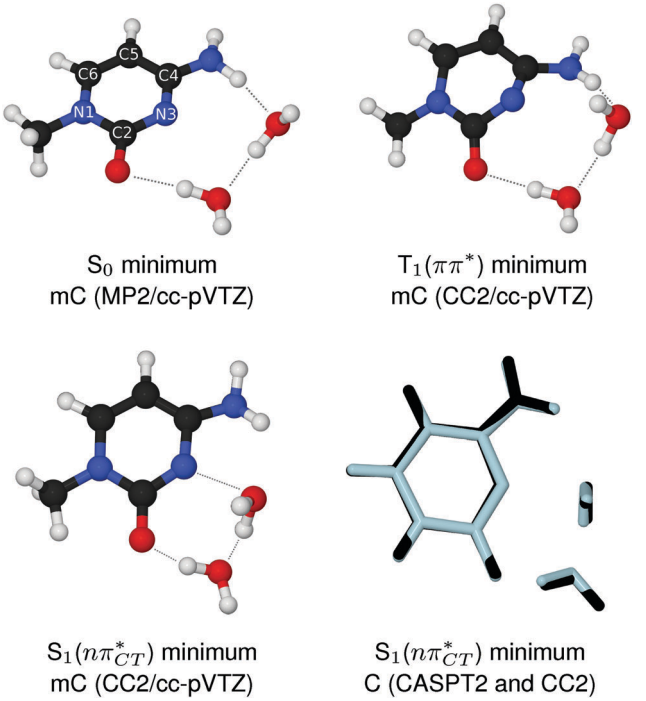

Fig. 1 Stationary points optimized for the mC–$(H_2O)_2$ cluster using the CC2/cc-pVTZ and MP2/cc-pVTZ methods (ground state). Hydrogen bonds and the strong N3$\cdots$O interaction in the S_1 state are marked with dotted lines. The bottom right panel shows the comparison of the S_1 minima of the cytosine–$(H_2O)_2$ cluster optimized using the CASPT2/SA-CASSCF/6-31G* (black) and CC2/cc-pVTZ (light blue) methods.

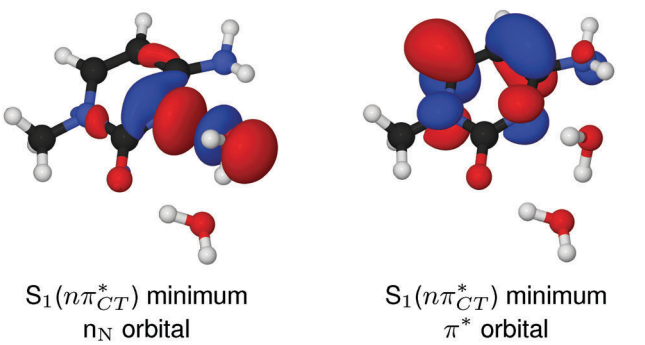

Fig. 2 The n_N and π* orbitals associated with the water–chromophore electron transfer process, which occurs in the vicinity of the S_1 minimum of the mC–$(H_2O)_2$ cluster.

This journal is © the Owner Societies 2017

Published on 21 junio 2017. Downloaded by Fail Open on 23/07/2025 9:10:29.

Table 1 Vertical excitation energies (in eV) of the considered mC–$(H_2O)_2$ cluster, computed using the CC2/cc-pVTZ method assuming the MP2/cc-pVTZ optimized S_0 minimum energy structure

State	Transition	E_{exc}/[eV]	f_{osc}	λ/[nm]
mC–$(H_2O)_2$ cluster				
S_1	$\pi\pi^*$	4.88	7.41×10^{-2}	254.1
S_2	$n_N\pi^*$	5.23	6.49×10^{-3}	237.1
S_3	$\pi\pi^*$	5.48	0.170	226.2
S_4	$n_O\pi^*$	5.56	9.09×10^{-4}	223.0

picoseconds after UV-excitation at 267 nm, while the further excited-state dynamics occurred on the surface of a dark excited electronic state.[27] We would like to emphasize here that further details related to the population of the $^1n\pi^*_{CT}$ state could be obtained by nonadiabatic molecular dynamics simulations, involving a possibly larger mC–water cluster. However, based on our tentative calculations (Fig. S3, ESI†), we assume that the $^1n\pi^*_{CT}$ excitation can be populated in a very similar manner to the case of microhydrated adenine.[21] It was also shown that only a minor fraction of the excited-state population in aqueous cytidine may reach the $\pi\pi^*/S_0$ conical intersection in a ballistic manner, without populating the long-lived dark state.[28]

Since this $^1n\pi^*_{CT}$ excitation has a low oscillator strength (3.4×10^{-4} in the S_1 minimum), it might be the long-lived dark state observed independently by Hare *et al.*[18] and Quinn *et al.*[16,17] Therefore, we calculated harmonic vibrational frequencies in the $S_1(n\pi^*_{CT})$ minimum of the mC–$(H_2O)_2$ cluster, substituting all mobile protons with deuterium. These calculations revealed a distinctive and intense IR absorption band at 1566 cm^{-1} that is in excellent agreement with the experimental value of 1574 cm^{-1} (see the overlaid spectra in Fig. 3).[16,17] This band corresponds to the C=O stretching motion and its characteristic broadening in the TR-IR measurements is most likely the result of multiple hydrogen bonding patterns. The slight redshift of this characteristic band can be assigned to the slight elongation of the C2=O bond by merely 0.02 Å with respect to the ground state bond length of 1.24 Å. The excited-state elongation of the C=O bond is much more pronounced in the gas phase, where the minimum-energy geometry of the biradical $S_1(n\pi^*)$ state[2–4] is characterized by a C2–O single bond of 1.42 Å (according to our CC2 calculations). The resulting C2–O vibration of isolated mC is thus significantly redshifted, but nearly unobservable experimentally owing to generally very low transition moments of C–O vibrations. Therefore, it becomes evident that the lowest lying $n\pi^*$ states of mC in the gas phase and bulk water are remarkably different from one another in terms of both properties and spectral signatures.

The detailed assignment of all the TR-IR bands from ref. 16 is given in Table 2. The simulations of harmonic vibrational frequencies in the $S_1(n\pi^*_{CT})$ state indicate that two more absorption bands should be expected within the investigated frequency interval. These frequencies correspond to C5–C6 (1471 cm^{-1}) and C4=C5 (1608 cm^{-1}) stretchings and can be assigned to the two outermost TR-IR absorption signals. It seems that a fourth TR-IR absorption signal was recorded experimentally

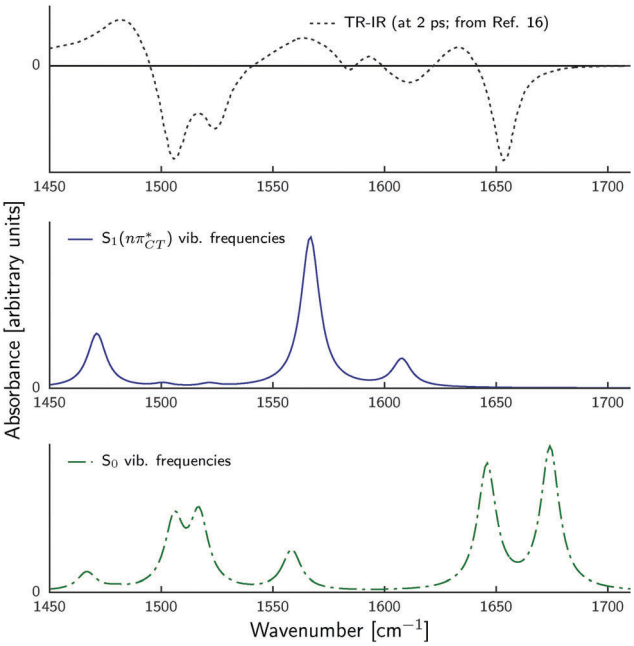

Fig. 3 IR spectra calculated for the mC–$(H_2O)_2$ cluster in the minimum of the $S_1(n\pi^*_{CT})$ state (middle; blue) and for mC molecule in the electronic ground state (bottom; green), using CC2/cc-pVTZ and B2PLYP(C-PCM)/def2-TZVPPD methods respectively. The digitalized TR-IR spectrum (at 2 ps) from ref. 16 is shown at the top of the graph.

Table 2 Positions of experimental vibrational bands from the digitalized TR-IR spectrum (at 2 ps) found in ref. 16 (middle column), along with the harmonic vibrational frequencies (right column) calculated in the $S_1(n\pi^*_{CT})$ minimum (CC2/cc-pVTZ) and the electronic ground-state (B2PLYP/def2-TZVPPD+C-PCM). The assignment to specific vibrational modes is presented in the left column

Vibration type	Experiment (TR-IR)[16]	Theory (harmonic)
Absorption bands (in cm^{-1})		
C5–C6 stretching	1482	1471
C=O stretching	1574	1566
C4=C5 stretching	1633	1608
Bleaching bands (in cm^{-1})		
C4=N3 stretching	1506	1506
C4–N(H_2) stretching	1524	1517
C4–C5 stretching	1584	1558
C=O stretching	1611	1645
C5=C6 stretching	1653	1674

at approximately 1595 cm^{-1}; however, we anticipate that it belongs to the rather diffused C=O vibrational band at 1574 cm^{-1}, which is bisected by a weak bleaching band at 1584 cm^{-1}. We assigned this bleaching band to the C4–C5 stretching vibration, based on the simulations of harmonic vibrational frequencies for isolated mC in the electronic ground state, performed using the B2PLYP method and the C-PCM solvation model of bulk water. Comparison to the B2PLYP harmonic vibrational frequencies in the electronic ground-state also enables rather straightforward assignment of the two lower bleaching bands recorded experimentally at 1506 and 1524 cm^{-1} (see Table 2).

Published on 21 junio 2017. Downloaded by Fail Open on 23/07/2025 9:10:29.

The ground-state C═O vibration was previously assigned to the rightmost bleaching band in the TR-IR experiments (1653 cm^{-1}). However, according to the B2PLYP harmonic vibrational frequencies, we propose that the bleaching band at $\approx$1611 cm^{-1} should be ascribed to the C═O stretching mode, while the negative TR-IR signal at 1653 cm^{-1} corresponds to C5═C6 stretching vibration. This can also be inferred from the experimental IR spectra measured by Keane *et al.*,[16,17] since C═O vibration bands are usually significantly broadened by interactions with water molecules and the rightmost bleaching band at 1653 cm^{-1} is a very sharp signal. The previous, presumably incorrect assignment of these bleaching bands was done based on the results of gas phase Hartree–Fock calculations, which did not reproduce the experimental IR spectrum even in a qualitative manner.

The previous excited-state configuration interaction singles (CIS) simulations of isolated mC yielded two excited-state geometries having either a significantly puckered pyrimidine ring or the C═O bond tilted out of the ring plane.[16] These S_1 state geometries were not found in later simulations of cytosine performed using more accurate methods,[2,4,5,29] which explains why the CIS vibrational frequency calculations were insufficient to enable the correct interpretation of the experimental data.[16] In fact, according to Brillouin's theorem, the CIS method lacks the electron correlation and the description of excited-state PE surfaces, geometries and vibrational frequencies is often qualitatively incorrect. Our results demonstrate that not only is the proper description of dynamical electron correlation essential, but also consideration of explicit solvation effects is often necessary to reproduce the character of challenging electronic states and support the interpretation of aqueous phase TR-IR experiments.

In order to provide solid proof that the dark state observed in the experiments of Keane *et al.*[16,17] can be assigned to the singlet $^1n\pi^*_{CT}$ state, similar considerations to those above are necessary for the lowest-lying triplet state, particularly since the nonadiabatic molecular dynamics simulations of isolated cytosine predicted triplet yields exceeding 20%.[5,6] Unfortunately, the simulations of vibrational frequencies in the T_1 minimum show that the absorption band corresponding to the C═O vibration can be found in a similar region to that in the $S_1(^1n\pi^*_{CT})$ state, namely at 1560 cm^{-1} (see the spectrum in Fig. S3 in the ESI†). Consequently, the T_1 and S_1 states of aqueous mC might be difficult to distinguish using solely TR-IR spectroscopy.

Additional information about the long-lived dark state can be obtained from time-resolved broadband TA-UV measurements performed by Ma *et al.*[27] In particular, *N*1-substituted cytosines in bulk water exhibit very weak and essentially featureless absorption in the spectral region between 350 and 600 nm, for time delays larger than 4 ps.[27] This is in good agreement with the excited-state UV-vis absorption spectrum simulated for the mC–$(H_2O)_2$ cluster in the minimum of the $^1n\pi^*_{CT}$ state (Fig. 4), for which a broad and jagged absorption region is visible between 280 and 360 nm and nearly no absorption for wavelengths longer than 360 nm. In contrast, the simulated excited-state UV-vis absorption spectrum

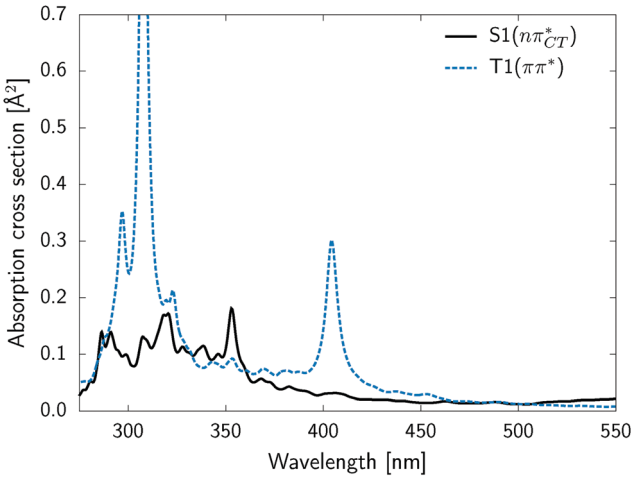

Fig. 4 Excited-state UV-vis absorption (ESA) spectra simulated in the minima of the two low-lying dark excited states ($^1n\pi^*_{CT}$ and $^3\pi\pi^*$), for the mC–$(H_2O)_2$ cluster (CC2/cc-pVTZ method).

of the $T_1(^3\pi\pi^*)$ state reveals a very distinct band centered at 400 nm (Fig. 4), which is not present in the spectra acquired by Ma *et al.*[27] Even though we expect this band to be broader in bulk environments, it would be an evident spectral feature in the TA-UV measurements if the triplet yields indeed exceeded 20%, as suggested by nonadiabatic molecular dynamics simulations of cytosine in the gas phase.[5,6] In addition, it should persist over longer time scales that are typical for triplet states (*i.e.* nanoseconds), whereas the excited-state lifetime of the dark state reported for aqueous mC is on the order of tens of picoseconds. These findings additionally support our assignment of the $^1n\pi^*_{CT}$ excitation to the long-lived dark state.

Very recently, Martinez-Fernandez *et al.*[30] proposed that the long-lived dark state could be assigned to the alternative $n_O\pi^*$ excitation, based on TD-CAM-B3LYP geometry optimizations and harmonic vibrational frequency simulations, and CASPT2/MM calculations. However, no explicit QM water molecules were considered in the CASPT2/MM scheme employed by the authors and, consequently, this approach was not capable of reproducing the character of the $^1n\pi^*_{CT}$ state and the WCET process. Even though the authors considered explicit QM water molecules at the TD-CAM-B3LYP level, these simulations yielded $n_O\pi^*$ and $n_N\pi^*$ excited-state geometries resembling the spurious CIS structures proposed earlier by Keane *et al.* (see the discussion above),[16] including the $n_O\pi^*$ geometry characterized by the C2═O bond tilted out of the ring plane. In contrast, the $^1n\pi^*_{CT}$ state was not reported at the TD-CAM-B3LYP level so far. Our attempts to optimize the analogous tilted $n_O\pi^*$ minimum-energy geometry for isolated mC at the more reliable CC2 level yielded only a structure having the C2–O (single) bond in plane with the aromatic ring. In addition, our CC2 simulations of the mC–$(H_2O)_2$ cluster indicate that the $n_O\pi^*$ lies 3.0 eV above the minimum of the $^1n\pi^*_{CT}$ state and becomes nearly inaccessible in the microhydrated chromophore. This energy difference is confirmed by additional EOM-CCSD calculations also performed including the explicit QM water molecules.

 This journal is © the Owner Societies 2017

Published on 21 junio 2017. Downloaded by Fail Open on 23/07/2025 9:10:29.

These results suggest that water has substantial influence on the balance between the $n_O\pi^*$ and $n_N\pi^*$ states in mC and the WCET effect may be observed only by employing a highly correlated QM method and including explicit water molecules described at the same level of theory as the chromophore moiety.

The very low triplet yields reported for cytidines in aqueous environments[18,27] might be the consequence of the $^1n\pi^*_{CT}$ state population which could substantially suppress intersystem crossing (ISC) to the triplet manifold. The strong O···N3 interaction in the S_1 minimum of the mC–$(H_2O)_2$ cluster significantly destabilizes $\pi\pi^*$ states both in the singlet and triplet manifolds. As a result, the $^3\pi\pi^*$ excitation becomes the T_2 state and lies 1.8 eV above the minimum of the $^1n\pi^*_{CT}$ state. Therefore, the corresponding $S_1 \rightsquigarrow T_2$ ISC is energetically inaccessible. In contrast, the energetically accessible T_1 state is of the same orbital character as the S_1 state, *i.e.* $n\pi^*_{CT}$, and the spin–orbit coupling between these states that amounts to merely 2.2 cm^{-1} is negligible. This indicates that the $S_1 \rightsquigarrow T_1$ ISC might be very inefficient in aqueous mC and the S_1 state might not be the precursor to triplet formation as suggested previously.[18]

Photoinduced electron transfer processes often result in a subsequent proton transfer in the direction of the displaced charge.[31,32] This phenomenon, also referred to as electron-driven proton transfer (EDPT), is responsible for the formation of S_1/S_0 conical intersections that are accessible with virtually no barrier in numerous biomolecular systems.[31,32] According to our calculations, a similar process may enable the radiationless deactivation of the $^1n\pi^*_{CT}$ state in the mC–$(H_2O)_2$ cluster. As shown in Fig. 5, the proton may be transferred from the positively charged H_2O^+ to the carbonyl oxygen atom, where the water molecule lying in-between serves as a proton relay. The two proton transfers occur in a nearly concerted manner and are associated with a low energy barrier of 0.21 eV (which is most likely overestimated due to the interpolation procedure). When the C═O···H–OH distance decreases below 1.1 Å, the $^1n\pi^*_{CT}$ and S_0 states become degenerate, enabling the radiationless deactivation of the photoexcited mC–$(H_2O)_2$ cluster. Geometry optimizations performed at the MR-CISD(4,3)/6-31G* level confirm that this conical intersection is available in both cytosine and mC. It is reasonable to assume that this EDPT conical intersection can be accessed only after the occurrence of the WCET process, since no equivalent S_1/S_0 state crossing could be located on the surfaces of states other than the $^1n\pi^*_{CT}$ excitation.

After the photodeactivation through the EDPT conical intersection to the ground electronic state, the electron might be transferred back to the water cluster and the initial photoproducts would comprise of protonated mC and a hydroxide anion. Even though the intuitive backward proton transfer along the bridging H_2O molecule enables deprotonation and restoration of the initial form of the chromophore, the presence of the hydroxide anion may have additional compelling consequences for protonated and positively charged mC. In particular, protonation of the nucleobase enables nucleophilic additions to the aromatic ring, which would not occur otherwise.

The remarkably high mobility of hydroxide anions in aqueous solutions[33] might result in nucleophilic addition to the heteroaromatic ring and photodamage. From the resonance structures of protonated cytidine proposed based on the valence bond analysis of the CASSCF wave function (CASVB; see Fig. 6 and the ESI†), the excess positive charge may reside on the C2, C4 or C6 carbon atoms (see Fig. 1 for atom numbering). Consequently, a nucleophilic attack of the 2′-OH oxygen on the C2 carbon atom may yield oxazolidinone, which was reported as the major photoproduct in UV-irradiation experiments of α-ribocytidine.[9–13] If the nucleophilic attack of the hydroxide anion occurs at the C4

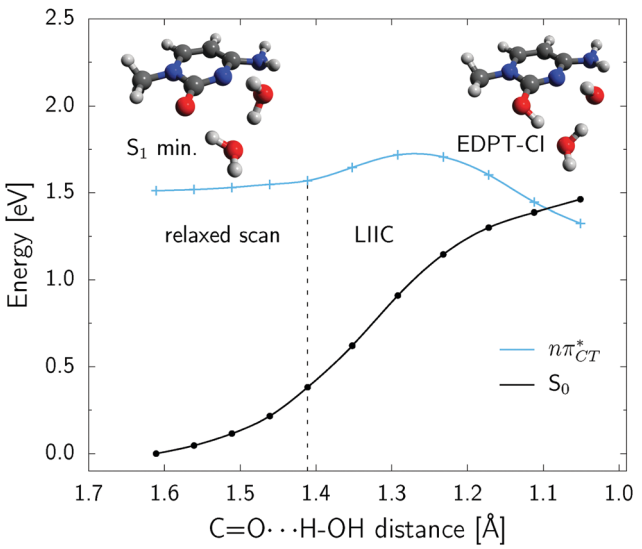

Fig. 5 Potential energy profile presenting the electron-driven proton transfer mechanism which may occur on the $^1n\pi^*_{CT}$ hypersurface. All energies and the geometries corresponding to the relaxed scan from the S_1 minimum along the C═O···H–OH distance were obtained at the CC2/cc-pVTZ level. Linear interpolation in internal coordinates (LIIC) between the last geometry of the relaxed scan and the conical intersection geometry obtained using the MR-CISD(4,3)/6-31G* method.

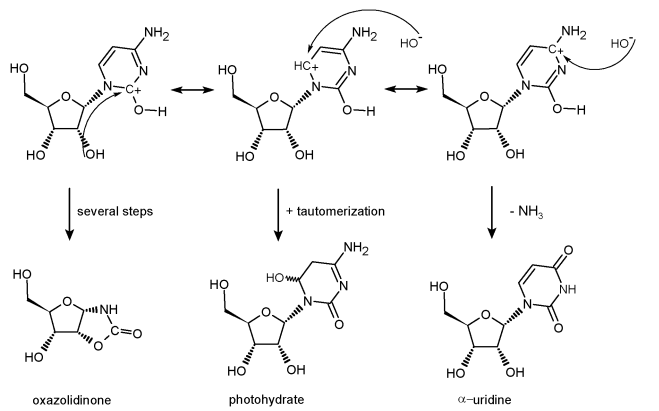

Fig. 6 Possible resonance structures of protonated cytidine suggest that the excess positive charge may be located on C2, C4 or C6 carbon atoms. These structures may be used to explain the variety of photoproducts observed by Powner *et al.*[9–13] in UV-irradiation experiments of α-ribocytidine, *i.e.* oxazolidinone, cytidine photohydrates and C to U conversion.

Published on 21 junio 2017. Downloaded by Fail Open on 23/07/2025 9:10:29.

position, the subsequent elimination of ammonia may result in C to U conversion. In contrast, if the hydroxide anion migrates to the near proximity of the C6 atom, the subsequent addition reaction may lead to the formation of cytidine photohydrate. It is worth noting that already in 1972 Burr *et al.*[34] hypothesized that the crucial intermediate in the photohydration reaction might be a hidden nπ* state or a singlet excited water–pyrimidine complex. Our assignment of the $^1n\pi^*_{CT}$ excitation of aqueous mC as a key intermediate state is in excellent agreement with both these suggestions.

In conclusion, our simulations of vibrational frequencies and excited-state absorption in the UV spectral range performed for the mC–$(H_2O)_2$ cluster enable the reinterpretation of time-resolved spectroscopic data acquired for aqueous cytidines within the past ten years. Our results provide solid proof that the long-lived dark state observed in these experiments may be a singlet nπ* state characterized by pronounced water-to-chromophore charge transfer (WCET) and a strong $H_2O\cdots N3$ interaction. Herein, we show for the first time that the $^1n\pi^*_{CT}$ excitation is accessible in a biologically relevant tautomer of a nucleobase and that it has intriguing consequences for the overall photoreactivity of the corresponding nucleosides. Microsolvation of mC suggests that water destabilizes the $n_O\pi^*$ state available in the isolated chromophore and the $^1n\pi^*_{CT}$ excitation is predominantly associated with the n_N molecular orbital. The EDPT conical intersection with the S_0 state may be readily accessed on the $^1n\pi^*_{CT}$ hypersurface of the mC–$(H_2O)_2$ cluster and is yet another example of a state crossing formed by direct interactions with solvent molecules. The initial photoproducts accessed *via* this conical intersection, namely the protonated mC and the OH^- anion, additionally elucidate photohydration, C to U conversion, and oxazolidinone formation reactions. Therefore, the assignment of the long-lived dark state in aqueous cytidine to the $^1n\pi^*_{CT}$ excitation serves as a single explanation for numerous previously unexplained experimental observations. Consistent with the most recent findings for 2-aminooxazole and adenine,[21–23,25,26] this study confirms that inclusion of explicit QM water molecules treated at the same level as the studied chromophore molecule is often essential to understand mechanistic details of its aqueous phase photochemistry. It should be underscored that the WCET process discussed here cannot be described by implicit solvation models or through electrostatic embedding (*i.e.* QM/MM) schemes.

Computational methods

The ground-state equilibrium geometry of the mC–$(H_2O)_2$ cluster was optimized at the MP2/cc-pVTZ level,[35] whereas the minimum energy geometries of the S_1 and T_1 states were obtained using the CC2/cc-pVTZ method.[36,37] Further simulations of vertical excitation energies, excited-state PE surfaces and frequencies, and excited-state absorption spectra were performed at the CC2/cc-pVTZ level of theory. To test the applicability of the CC2 method for the above mentioned purposes we performed additional CASPT2/SA-CASSCF(6,5)/cc-pVTZ-DK and EOM-CCSD/TZVP benchmark calculations. These higher level calculations confirmed that the CC2 method provides a reliable description of PE surfaces outside the Franck–Condon region of mC, which is consistent with our most recent investigations performed for isocytosine.[38] We suggested previously that it might be necessary to use multireference wave function methods in the vicinity of $n\pi^*/S_0$ conical intersections,[38] and the MR-CISD(4,3)/6-31G* approach was applied for the optimization of the EDPT conical intersection. More detailed description of the computational methods is provided in the ESI.†

Acknowledgements

We thank Prof. John D. Sutherland, Dr Jan Mewes and Prof. Wolfgang Zinth for fruitful discussions. This work was supported by a grant from the Simons Foundation (494188 to R. S.). J. S. acknowledges support from the Praemium Academiae. Financial support from the National Science Centre (DEC-2016/23/B/ST4/01048 to R. W. G.) and a statutory activity subsidy from the Polish Ministry of Science and Higher Education for the Faculty of Chemistry of Wrocław University of Science and Technology, as well as computational grants from the Interdisciplinary Centre for Mathematical and Computational Modelling (ICM, Grant No. G53-28) and the Wrocław Centre of Networking and Supercomputing (WCSS), are gratefully acknowledged.

References

1 N. Ismail, L. Blancafort, M. Olivucci, B. Kohler and M. A. Robb, *J. Am. Chem. Soc.*, 2002, **124**, 6818–6819.
2 M. Barbatti, A. J. A. Aquino, J. J. Szymczak, D. Nachtigallová, P. Hobza and H. Lischka, *Proc. Natl. Acad. Sci. U. S. A.*, 2010, **107**, 21453–21458.
3 K. Kleinermanns, D. Nachtigallová and M. S. de Vries, *Int. Rev. Phys. Chem.*, 2013, **32**, 308–342.
4 M. Barbatti, A. J. A. Aquino, J. J. Szymczak, D. Nachtigallová and H. Lischka, *Phys. Chem. Chem. Phys.*, 2011, **13**, 6145–6155.
5 M. Richter, P. Marquetand, J. González-Vázquez, I. Sola and L. González, *J. Phys. Chem. Lett.*, 2012, **3**, 3090–3095.
6 S. Mai, P. Marquetand, M. Richter, J. González-Vázquez and L. González, *ChemPhysChem*, 2013, **14**, 2920–2931.
7 F.-T. Liu and N. C. Yang, *Biochemistry*, 1978, **17**, 4877–4885.
8 R. J. Boorstein, T. P. Hilbert, R. P. Cunningham and G. W. Teebor, *Biochemistry*, 1990, **29**, 10455–10460.
9 C. Anastasi, M. A. Crowe, M. W. Powner and J. D. Sutherland, *Angew. Chem., Int. Ed.*, 2006, **45**, 6176–6179.
10 C. Anastasi, M. A. Crowe and J. D. Sutherland, *J. Am. Chem. Soc.*, 2007, **129**, 24–25.
11 M. W. Powner, C. Anastasi, M. A. Crowe, A. L. Parkes, J. Raftery and J. D. Sutherland, *ChemBioChem*, 2007, **8**, 1170–1179.
12 M. Powner and J. Sutherland, *ChemBioChem*, 2008, **9**, 2386–2387.
13 M. W. Powner, B. Gerland and J. D. Sutherland, *Nature*, 2009, **459**, 239–242.

 This journal is © the Owner Societies 2017

Published on 21 junio 2017. Downloaded by Fail Open on 23/07/2025 9:10:29.

14 S. De Camillis, J. Miles, G. Alexander, O. Ghafur, I. D. Williams, D. Townsend and J. B. Greenwood, *Phys. Chem. Chem. Phys.*, 2010, **17**, 23643–23650.
15 K. Rottger, H. J. B. Marroux, H. Bohnke, D. T. J. Morris, A. T. Voice, F. Temps, G. M. Roberts and A. J. Orr-Ewing, *Faraday Discuss.*, 2016, **194**, 683–708.
16 P. M. Keane, M. Wojdyla, G. W. Doorley, G. W. Watson, I. P. Clark, G. M. Greetham, A. W. Parker, M. Towrie, J. M. Kelly and S. J. Quinn, *J. Am. Chem. Soc.*, 2011, **133**, 4212–4215.
17 S. Quinn, G. W. Doorley, G. W. Watson, A. J. Cowan, M. W. George, A. W. Parker, K. L. Ronayne, M. Towrie and J. M. Kelly, *Chem. Commun.*, 2007, 2130–2132.
18 P. M. Hare, C. E. Crespo-Hernández and B. Kohler, *Proc. Natl. Acad. Sci. U. S. A.*, 2007, **104**, 435–440.
19 J. Cadet and P. Vigny, *Bioorganic Photochemistry: Photochemistry and the nucleic acids*, Wiley, New York, 1990, ch. 1, vol. 1, pp. 1–272.
20 C. Salet, R. Bensasson and R. S. Becker, *Photochem. Photobiol.*, 1979, **30**, 325–329.
21 M. Barbatti, *J. Am. Chem. Soc.*, 2014, **136**, 10246–10249.
22 R. Szabla, J. Šponer and R. W. Góra, *J. Phys. Chem. Lett.*, 2015, **6**, 1467–1471.
23 R. Szabla, R. W. Góra, M. Janicki and J. Šponer, *Faraday Discuss.*, 2016, **195**, 237–251.
24 R. Szabla, J. E. Šponer, J. Šponer, A. L. Sobolewski and R. W. Góra, *Phys. Chem. Chem. Phys.*, 2014, **16**, 17617–17626.
25 X. Wu, T. N. V. Karsili and W. Domcke, *ChemPhysChem*, 2016, **17**, 1298–1304.
26 S. Chaiwongwattana, M. Sapunar, A. Ponzi, P. Decleva and N. Došlić, *J. Phys. Chem. A*, 2015, **119**, 10637–10644.
27 C. Ma, C. C.-W. Cheng, C. T.-L. Chan, R. C.-T. Chan and W.-M. Kwok, *Phys. Chem. Chem. Phys.*, 2015, **17**, 19045–19057.
28 A. J. Pepino, J. Segarra-Martí, A. Nenov, R. Improta and M. Garavelli, *J. Phys. Chem. Lett.*, 2017, **8**, 1777–1783.
29 J. González-Vázquez and L. González, *ChemPhysChem*, 2010, **11**, 3617–3624.
30 L. Martínez-Fernández, A. J. Pepino, J. Segarra-Martí, J. Jovaišaitė, I. Vaya, A. Nenov, D. Markovitsi, T. Gustavsson, A. Banyasz, M. Garavelli and R. Improta, *J. Am. Chem. Soc.*, 2017, **139**, 7780–7791.
31 A. L. Sobolewski, W. Domcke and C. Hättig, *Proc. Natl. Acad. Sci. U. S. A.*, 2005, **102**, 17903–17906.
32 A. Sobolewski and W. Domcke, *ChemPhysChem*, 2006, **7**, 561–564.
33 M. E. Tuckerman, D. Marx and M. Parrinello, *Nature*, 2002, **417**, 925–929.
34 J. G. Burr, E. H. Park and A. Chan, *J. Am. Chem. Soc.*, 1972, **94**, 5866–5872.
35 F. Weigend and M. Häser, *Theor. Chem. Acc.*, 1997, **97**, 331–340.
36 C. Hättig, *Adv. Quantum Chem.*, 2005, **50**, 37–60.
37 C. Hättig and F. Weigend, *J. Chem. Phys.*, 2000, **113**, 5154–5161.
38 R. Szabla, R. W. Góra and J. Šponer, *Phys. Chem. Chem. Phys.*, 2016, **18**, 20208–20218.